

Facile Synthesis of Ni-Co Double Hydroxide on Carbonized Cotton Cloth for High Performance Supercapacitor

Yanni Shen¹, Xueli Miao¹, Dandan Song¹, Yanting Li¹, Yuning Qu¹, Jianguo Yu¹, Jiajun Tang², Hao Qin¹, Lili wang^{1,*}, Jiahao Ren¹, Bing Wang^{1,*}

¹ School of Environment and Chemical Engineering, State Key Laboratory of Separation Membranes and Membrane Processes, Tianjin Polytechnic University, 399 Binshui West Road, Tianjin 300387, P. R. China

² School of Materials Science and Engineering and Tianjin Key Laboratory of Fiber, Tianjin Polytechnic University, Tianjin 300387, China

*E-mail: wanglili@tjpu.edu.cn / cnbingwang@tjpu.edu.cn

Received: 20 November 2018/ Accepted: 12 January 2019 / Published: 7 February 2019

A facile and novel one-step hydrothermal method was provided for the preparation of Ni-Co double hydroxides (NC-DH), which was directly grown on carbonized cotton cloth (CCC) and used as advanced binder-free electrodes for supercapacitors. The effect of different concentration of Ni²⁺ and Co²⁺ in the initial reactant (C-Ni-x-Co-y) on microstructure and electrochemical performance were studied. The results showed that flake-like structure grown uniformly under an appropriate concentration, which was benefit to improve the electrochemical performance. The electrochemical tests revealed that the C-Ni-4-Co-8 electrode displayed the maximum specific capacitance of 4.19 F cm⁻² when the current density was 5 mA cm⁻² and excellent rate capability maintained at 3.05 F cm⁻² even at the high current density of 80 mA cm⁻². The electrodes of Ni-Co double hydroxides anchored on flexible conductive substrates with excellent electrochemical properties could be obtained by cost-effective method, which could be ascribed as a highly promising potential electrode material for energy storage devices.

Keywords: Ni-Co double hydroxide, carbonized cotton cloth, hydrothermal method, supercapacitor.

1. INTRODUCTION

Searching for green renewable energy and efficient energy storage systems are important ways to solve the issues of environmental pollution and energy shortage. Supercapacitors have attracted much attention among the new energy-storage devices due to their characteristics of high power density, ultrafast power supply and long cycle life. Electrode materials as the core component of

supercapacitors have become a key factor for its development [1-5]. At present, carbon materials such as graphene, carbon nanotubes and activated carbon used as electrode materials have been widely reported because they have good charge/discharge cycling stability, excellent electronic conductivity, large specific surface area and non-toxicity [6-8]. However, carbon-based supercapacitors often show the relatively low specific capacitance and low energy density, and these problems have seriously limited their practical application in supercapacitors [9, 10]. Thus, transition-metal oxides/hydroxides with high theoretical specific capacitance, good redox activity and high energy density are extensively investigated, particularly, Ni-Co double hydroxides (NC-DH) have been considered to be the most competitive electrode materials [11-13]. It may reduce the hydrous content and increase crystallinity when the metal hydroxides were converted into oxides by high temperature annealing, which led to the deterioration of specific capacitance of metal oxides compared with their metal hydroxides [14, 15]. Moreover, the composites consisting of nickel and cobalt ions can offer richer charge storage than a single component, their morphology and structure may affect the ion-diffusion rate and electronic conductivity of active material prominently in supercapacitors [16]. For previous reports, the mesoporous nickel-cobalt layered double hydroxides were prepared through a chemical coprecipitation method, the gravimetric capacitance of this electrode was 1809 F g^{-1} at 1 A g^{-1} [17], the nickel-cobalt hydroxide nanoflakes grown on carbon nanotube were fabricated by the chemical precipitation process and the specific capacitance reached 1843 F g^{-1} at 0.5 A g^{-1} [18]. In conventional electrode fabrication process, electroactive materials are mixed with insulating binder and conductive agent in a certain ratio, then coated on metallic substrate which performed as current collectors. It will cause "dead surface", which means the electrolyte can not in contact with the active material sufficiently [19]. These additives hinder the diffusion of electrolyte and reduce the utilization efficiency of active substances, which leads to the decrease in the rate capability and cycle stability of the electroactive material. Hence, the effective strategy to solve these problems is to grow the active materials directly on conductive substrate as binder-free electrodes.

As we know, carbon cloth is widely used to enhance the electrochemical performance of supercapacitors as an inexpensive and conductive flexible substrate [20]. The three dimensional structures of carbon cloth are favorable to increase the electroactive surface of electrodes in contact with electrolyte and make the electrolyte ions easy to diffuse, which is helpful for promoting the transfer of electrons, and avoiding the appearance of "dead surface". Therefore, the carbon cloth exhibits good electrical conductivity and better cycle stability as a conductive flexible substrate [21-23].

In this paper, the high capacitance nickel-cobalt double hydroxides (NC-DH) grown on the carbonized cotton cloth (CCC) was reported, it was fabricated through the economical hydrothermal synthesis process and applied as binder-free electrodes for supercapacitors. The active materials grew uniformly on carbonized cotton cloth with better structure and morphology, which increased the amount of electroactive sites. The three dimensional frameworks of carbon cloth provided numerous accessible channels for electron transport and promoted the diffusion of electrolyte ions. Furthermore, the electrochemical performance was enhanced without using polymer binders or additives. The results showed controllable morphologies of NC-DH which grown on the CCC under different concentrations of Ni^{2+} and Co^{2+} . The specific capacitance of the product was 4.19 F cm^{-2} at the current density of 5

mA cm⁻² and the product also exhibited excellent rate capability, which implied its potential application in supercapacitors as the electrode materials.

2. EXPERIMENTAL

2.1 Materials

The cobalt chloride hexahydrate (CoCl₂·6H₂O), nickel chloride hexahydrate (NiCl₂·6H₂O) and hexamethylenetetramine (HMT) were purchased from Aladdin, and they were of analytical grade. Carbonized cotton cloth (CCC) was used as the substrate to deposit active materials. Deionized (DI) water was used to prepare all aqueous solutions.

2.2 Growth of NC-DH on CCC

The CCC was obtained by direct carbonization of the cotton cloth under flowing nitrogen atmosphere. Typically, the cotton cloth was cleaned ultrasonically in ethanol and deionized water for 30 min respectively, then vacuum-dried for 24 h. The cotton cloth was treatment at 800°C for 1 h under nitrogen atmosphere, which was placed in an electronic tube furnace to obtain the carbon cloth.

The growth of NC-DH on a CCC was achieved by one-step hydrothermal method. Both NiCl₂·6H₂O and CoCl₂·6H₂O with molar ratio of 1:2 at different concentrations, 20 mmol HMT and 50 mL DI water were mixed to form transparent solution. After that, a piece of CCC substrate with 1×1 cm² in geometric size was immersed into above solution under stirring for 30 min at room temperature. Then the reaction mixture was transferred into autoclave and heated at 100°C for 5 h. Subsequently, the CCC was taken out and washed with ethanol and DI water several times when the equipment cooled down to room temperature naturally. Finally, the composite was dried at 60 °C overnight. The product was denoted as C-Ni-x-Co-y with x representing the initial concentration of NiCl₂·6H₂O (mmol), y representing the initial concentration of CoCl₂·6H₂O (mmol). Different concentration of Ni²⁺ and Co²⁺ was designed to determine the morphologies of NC-DH.

2.3 Material characterization

The scanning electron microscopy (SEM, Hitachi S4800) was used to record the morphology of samples. The structures of materials were measured by X-ray diffraction (XRD, Bruker D8 Discover) with Cu K α radiation. The chemical composition and state of the composite were collected by X-ray photoelectron spectroscopy (XPS) with Al K α radiation.

2.4 Electrochemical characterization

All the electrochemical properties including cyclic voltammogram (CV) and galvanostatic charge/discharge curve (GCD) were carried out in a three-electrode cell with a CHI760E (CH Instruments, China) electrochemical workstation. The 2 M KOH aqueous solution was used as electrolyte, the working electrode was carbon cloth covered with NC-DH compound, platinum electrode acted as the counter electrode and Hg/HgO electrode was used as reference electrodes.

The capacitance of the single electrode could be evaluated using the following equation:

$$C = (I \times t) / (V \times S)$$

Where C is the areal capacity ($F \cdot \text{cm}^{-2}$), t is the discharge time (s), I is the discharge current (A), V is the discharge voltage range of the electrode (V), S (cm^2) is the area of CCC covered with active materials which as the electrode [11].

3. RESULTS AND DISCUSSION

3.1 Structural and surface morphological characterization

The formation process of NC-DH grown on the carbonized cotton cloth substrate is schematically illustrated in Fig. 1. The cotton cloth was firstly carbonized into carbon cloth, then NC-DH in situ grew on the CCC substrate through one-step hydrothermal method. The cotton cloth had better conductivity after carbonization, and surface wrinkles on carbon cloth were favorable for the growth of NC-DH and their robust adhesion.

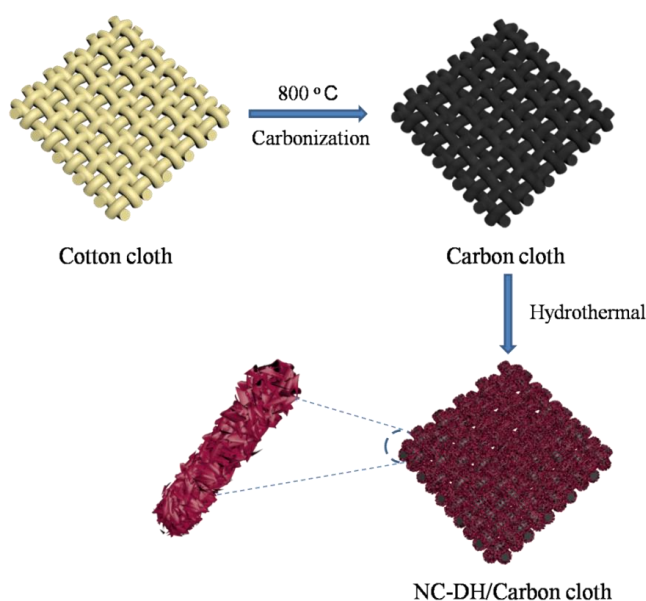


Figure 1. Schematic illustration of the fabrication of NC-DH onto carbonized cotton cloth.

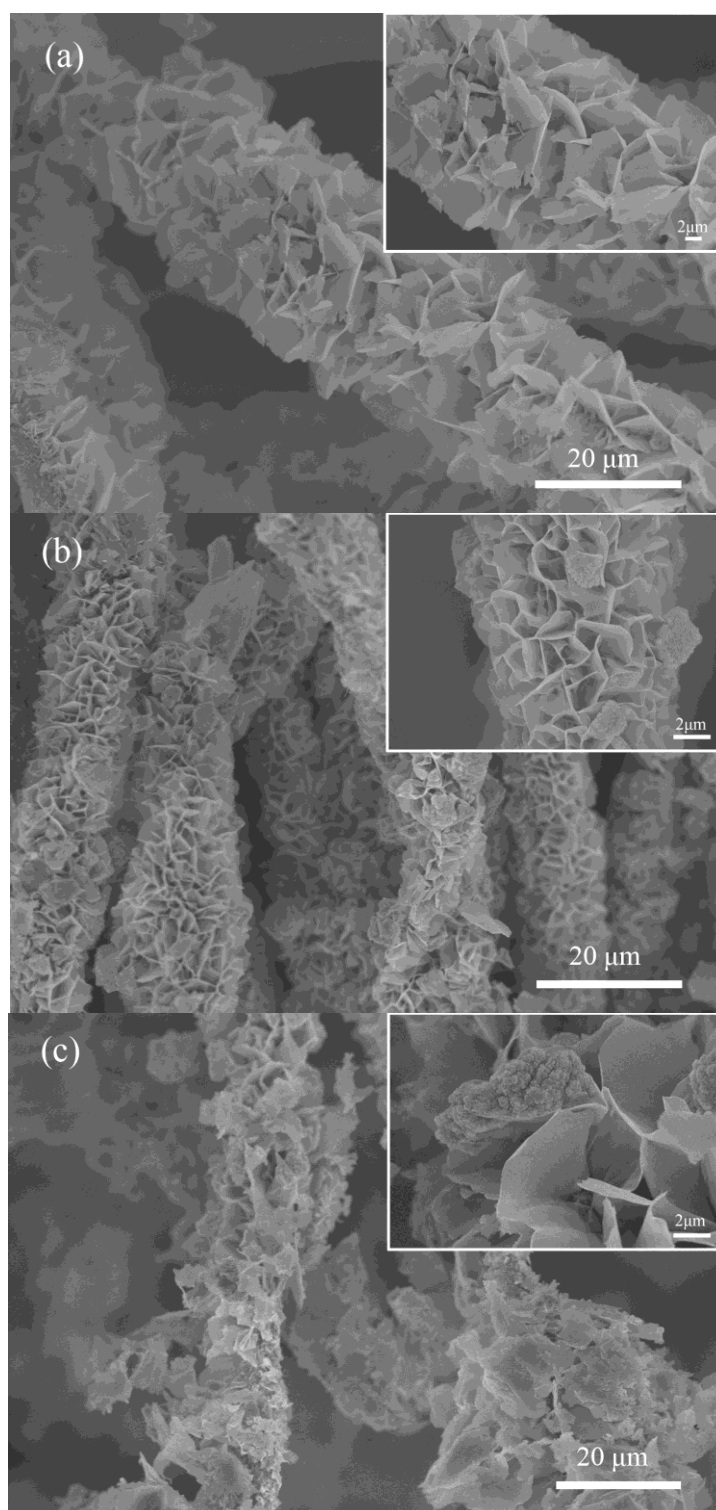


Figure 2. SEM images of C-Ni-x-Co-y prepared at different concentration: (a) C-Ni-3-Co-6, (b) C-Ni-4-Co-8, (c) C-Ni-5-Co-10.

During the reaction, HMT was decomposed to release NH_3 slowly under the heating condition, that made the solution became alkaline. The NH_3 formed amine complex with Ni^{2+} and Co^{2+} , and controlled the release rate of Ni^{2+} and Co^{2+} as complexing agent. Ni^{2+} and Co^{2+} could be easily adsorbed onto the surface of the substrate by electrostatic and strongly coupled in alkaline

environments [24]. Simultaneously, when the Ni^{2+} and Co^{2+} reacted with OH^- , the metal hydroxide monomers were first formed as nuclei and then converted into primary particles. As the primary particles aggregate, they underwent olation reaction with each other began to form NC-DH, and they were grown on CCC substrate in situ [25, 26].

The morphology of NC-DH grown on carbonized cotton cloth at different concentration was examined by SEM. Specifically, Fig. 2a shows that the product is uniformly grown on the CCC and has flake-like morphology with some cracks under the low concentration of Ni^{2+} and Co^{2+} . It can be seen that the flake-like structure becomes intact gradually as the concentration increases shown in Fig. 2b. The loosely packed structure provides large surface area that may allow electrolyte ions easy to diffuse and promote the electron transport. As indicated in Fig. 2c, the active substance grown on the carbon cloth are broken under high concentration of Ni^{2+} and Co^{2+} , which might lead to the decline in electrochemical performance.

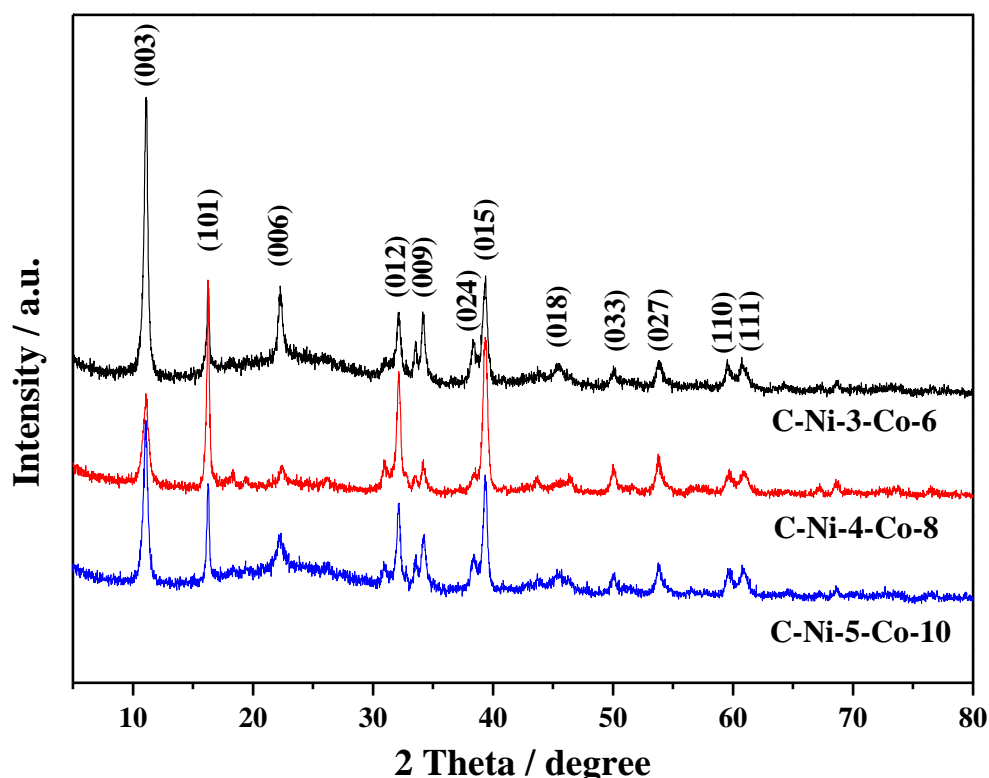


Figure 3. XRD patterns of C-Ni-x-Co-y synthesized at different initial concentrations.

The structure of the composite was analyzed using X-ray diffraction. Fig. 3 shows the XRD patterns of the composite synthesized by controlling the amount of Ni^{2+} and Co^{2+} in the initial reactants. The diffraction peaks of the product can be well indexed to the (003), (006), (009), (012), (015), (018), (110) and (111) plane reflection of hydrotalcite-like materials, indicating that the formation of NC-DH [24-27]. In addition, the peaks at around 17°, 37°, 50°, 54° correspond to the (101), (024), (033) and (027) planes of cobalt hydroxide chloride, respectively (JCPDS No. 73-2134). Since the concentration of cobalt was relatively large than nickel, hydroxide radicals were depleted

after the formation of metal hydroxide, some of the chloride radicals began to bond with cobalt ions, which may affect the morphology and phase of the product [15, 26].

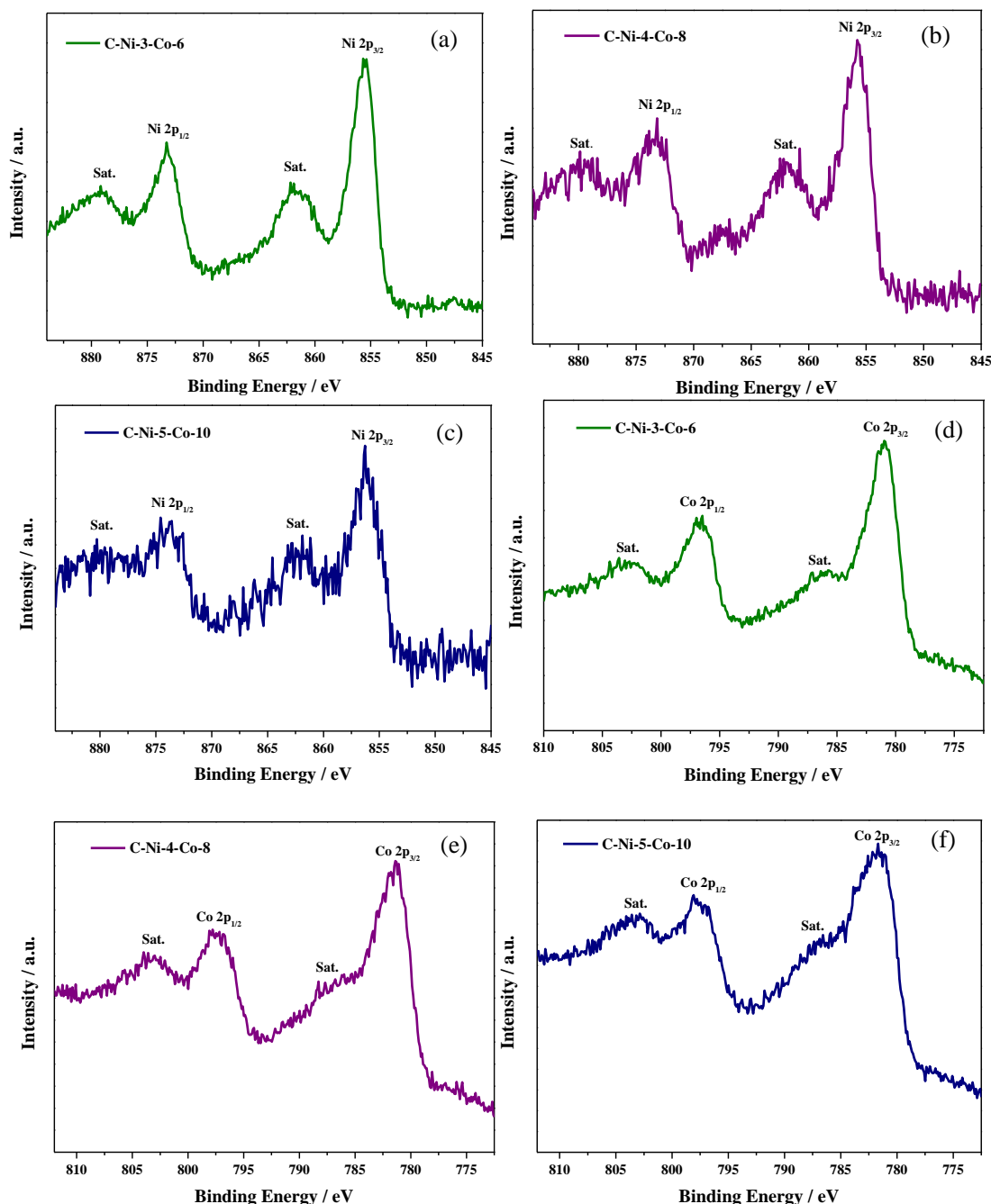
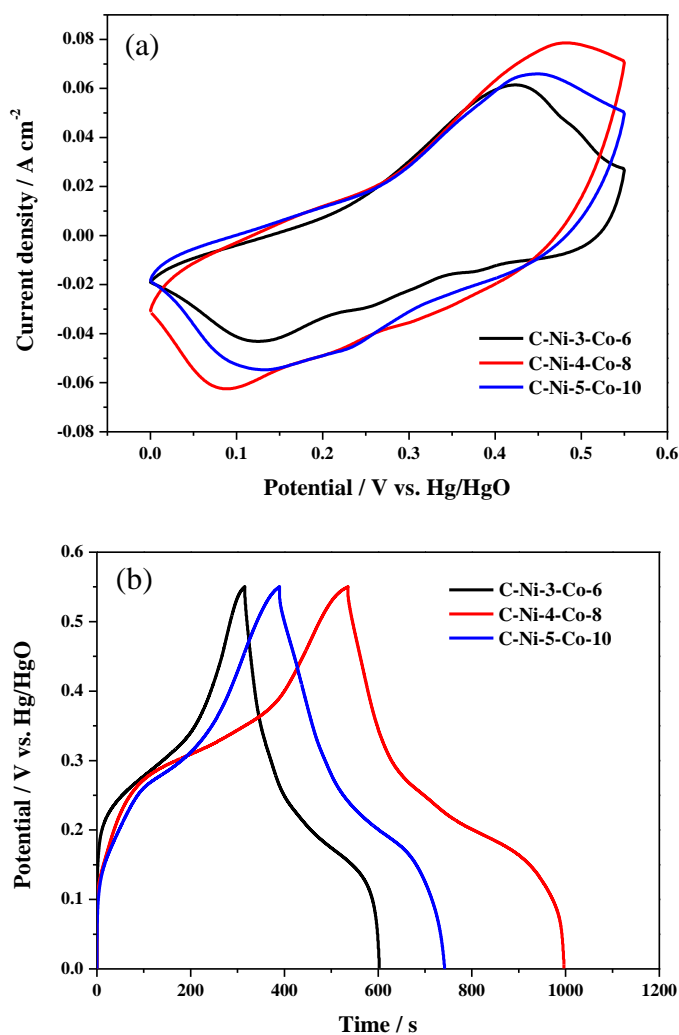


Figure 4. (a-c) Ni 2p and (d-f) Co 2p XPS spectra of C-Ni-x-Co-y electrodes.

To obtain further information on the chemical composition of samples, XPS measurements were performed. As displayed in Fig. 4, for XPS spectrum of Ni 2p, all the spectra reveal two spin-orbit doublets. The evident peaks at 873.3 and 855.6 eV represent the Ni 2p_{1/2} and Ni 2p_{3/2} of the C-Ni-3-Co-6, respectively (Fig. 4a), 873.4 and 855.7 eV represent the Ni 2p_{1/2} and Ni 2p_{3/2} of the C-Ni-4-Co-8, respectively (Fig. 4b), 873.7 and 856.2 eV represent the Ni 2p_{1/2} and Ni 2p_{3/2} of the C-Ni-5-Co-10, respectively (Fig. 4c). Simultaneously, two shakeup satellite peaks (indicated as “Sat”) can be seen

from the spectra, and all the peaks are ascribed to Ni²⁺ [11, 19]. Meanwhile, similar results can be observed from the XPS spectrum of Co 2p. The two spin-orbit doublets of C-Ni-3-Co-6 at 796.8 eV (Co 2p_{1/2}) and 780.8 eV (Co 2p_{3/2}) are shown in Fig. 4d, the peaks of C-Ni-4-Co-8 at 797.5 eV (Co 2p_{1/2}) and 781.4 eV (Co 2p_{3/2}) are revealed in Fig. 4e, and the peaks of C-Ni-5-Co-10 located at 797.7 eV (Co 2p_{1/2}) and 781.7 eV (Co 2p_{3/2}) are displayed in Fig. 4f. Besides, in all the XPS spectra of Co 2p, the satellite line intensity is pretty low which means the co-existence of Co²⁺ and Co³⁺ in the samples [26, 28]. The results show that the NC-DH has successfully grown on carbonized cotton cloth, which are consistent well with that of XRD analyses.

3.2 Electrochemical performance



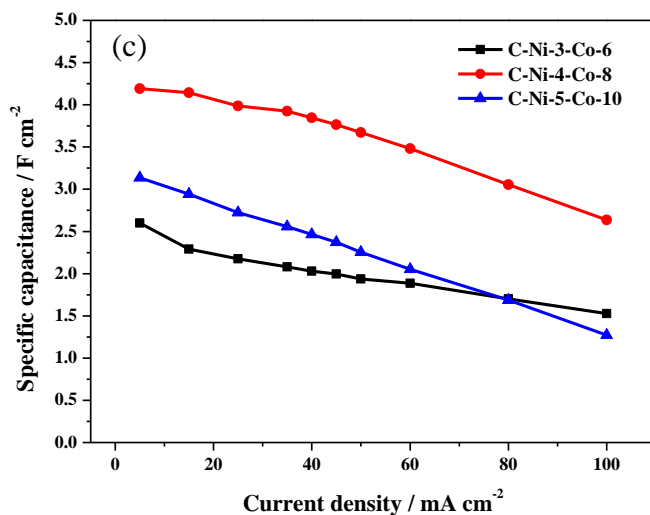
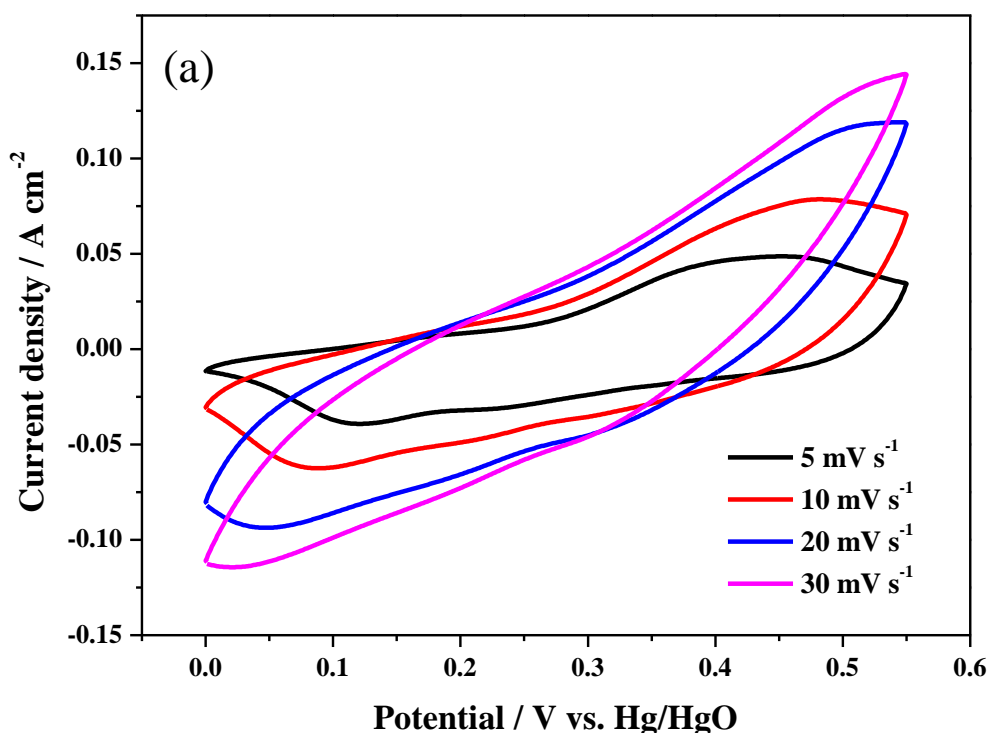


Figure 5. Electrochemical characterization of the C-Ni-x-Co-y electrodes in 2 M KOH: (a) CV curves obtained at 10 mV s⁻¹, (b) galvanostatic charge/discharge curves at 5 mA cm⁻², (c) capacitance retentions.

The electrochemical properties of the NC-DH grown on CC as supercapacitor electrodes were evaluated by the cyclic voltammogram (CV) and galvanostatic charge/discharge curve (GCD). Fig. 5a illustrates the CV curves of composites prepared at different concentration of Ni²⁺ and Co²⁺, the measurement was tested at a scan rate of 10 mV s⁻¹. A pair of well-defined redox peaks can be seen between 0 and 0.55 V, indicating that the capacitive characteristics are mainly influenced by the redox reaction [19, 29]. As the initial concentration of nickel and cobalt increased, the morphology of the material changed, resulting in the difference in electrochemical properties. The curve area increased at first but then decreased, which means the C-Ni-4-Co-8 electrode could store a larger amount of charge. As shown in Fig. 5b, the GCD measurement was carried out at a current density of 5 mA cm⁻².



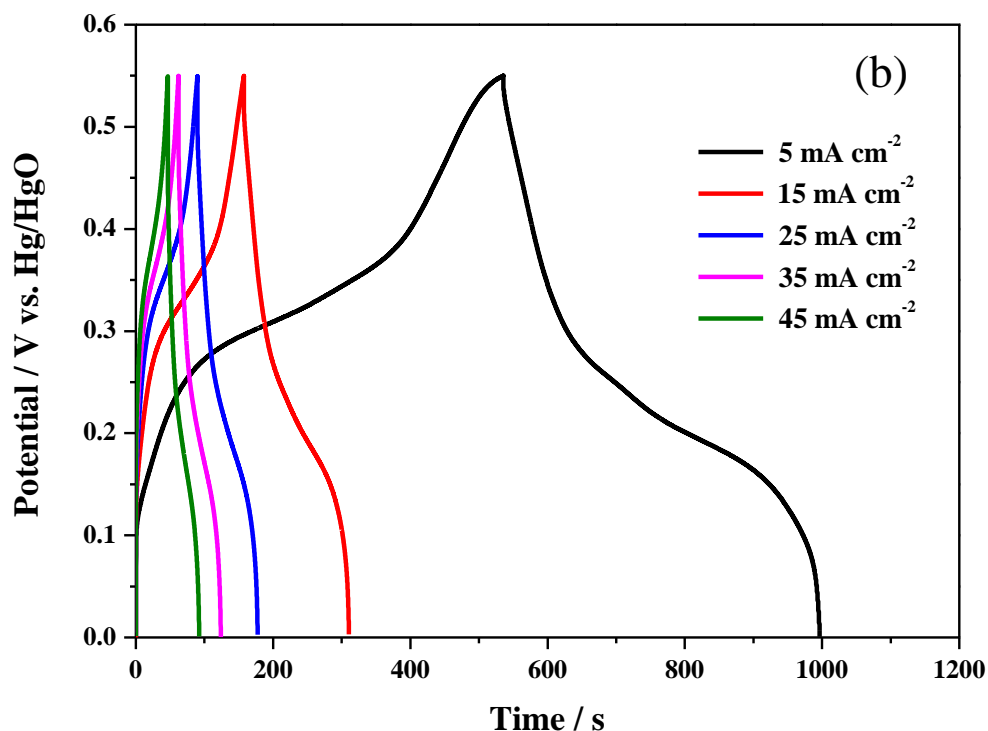


Figure 6. Electrochemical performances of the C-Ni-4-Co-8 electrode in 2 M KOH: (a) CV curves obtained at different scan rates, (b) galvanostatic charge/discharge curves obtained at various current densities.

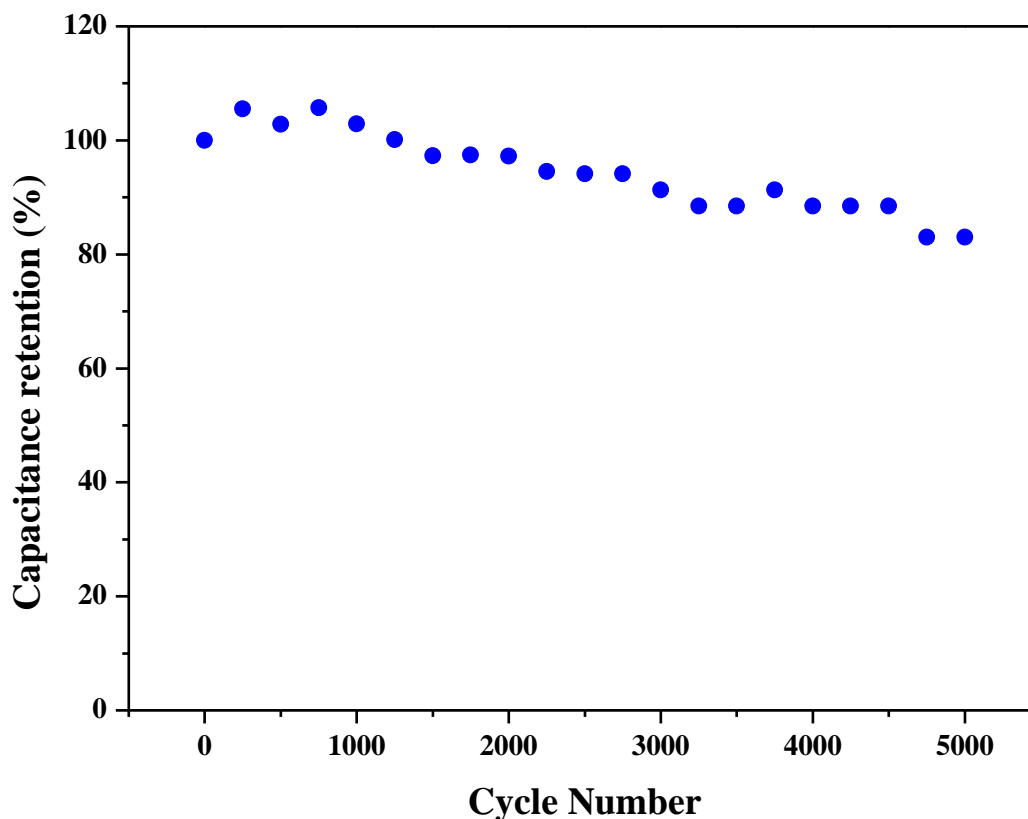
The well-defined plateaus observed in the potential window of 0-0.55 V suggest the faradaic characteristic of the electrodes, which are consistent with the CV tests [16, 27, 28, 30]. At the same current density, C-Ni-4-Co-8 electrode displayed a maximum capacitance as high as 4.19 F cm^{-2} . This result may be associated with the different initial concentration of Ni^{2+} and Co^{2+} under the same ratio of Ni/Co. The morphology of the active substance was affected by the variation in concentration. The modicum and over dosage of Ni^{2+} and Co^{2+} lead to the growth of NC-DH shattered and incomplete, it may affect the redox reaction of active materials and electrolyte ion diffusion. Therefore, the performance of C-Ni-4-Co-8 electrode was better than the C-Ni-3-Co-6 and the C-Ni-5-Co-10. Fig. 5c displays the variation of the specific capacitances at different current density for C-Ni-x-Co-y electrodes. As the current density increased, the specific capacitance of electrodes gradually decreased. Notably, the capacitances retention of C-Ni-3-Co-6, C-Ni-4-Co-8 and C-Ni-5-Co-10 electrodes were 58% , 62% and 41% , respectively, even the current density reached 100 mA cm^{-2} , which exhibited a favourable rate capability.

The CV profiles and GCD curves of the C-Ni-4-Co-8 electrode were tested and the results were provided in Fig. 6. Fig. 6a presents the CV curves of the electrode in the scan rate of 5-30 mV s^{-1} . It can be found that when the scan rate was increased, the anodic and cathodic peaks shifted toward both sides, respectively. The reason was that the ion-transfer resistance was decreased and ion-diffusion was accelerated as the scan rate increased [31]. The areal capacity of the C-Ni-4-Co-8 electrode were calculated according to Fig. 6b, which reached 4.19, 4.14, 3.98, 3.93 and 3.76 F cm^{-2} at various current densities of 5, 15, 25, 35 and 45 mA cm^{-2} , respectively. It implied the electrode materials had higher specific capacitance than other electrodes under large current densities (Table. 1).

Table 1. Comparison of electrochemical performance of different electrodes with the C-Ni-4-Co-8 electrode.

Samples	Capacitance	Rate performance
MnO ₂ nanosheet arrays on carbon cloth [32]	2.16 F cm ⁻² at 5 mA cm ⁻²	47% from 5 to 20 mA cm ⁻²
N-doped carbon cloth [33]	1.2 F cm ⁻² at 8 mA cm ⁻²	65% from 4 to 20 mA cm ⁻²
Co ₃ S ₄ nanosheet arrays [34]	2.69 F cm ⁻² at 4 mA cm ⁻²	73% from 4 to 20 mA cm ⁻²
Co _x Ni _{1-x} (OH) ₂ /NiCo ₂ S ₄ nanotube array [35]	2.86 F cm ⁻² at 4 mA cm ⁻²	84% from 4 to 20 mA cm ⁻²
Ni-Co selenide nanorod array on carbon fiber paper [36]	2.61 F cm ⁻² at 4 mA cm ⁻²	75% from 4 to 20 mA cm ⁻²
C-Ni-4-Co-8 electrode [this work]	4.19 F cm ⁻² at 5 mA cm ⁻²	95% from 5 to 25 mA cm ⁻²

Cycling stability is one of the key performance indicators of supercapacitors. The cycling stability of the C-Ni-4-Co-8 electrode was conducted by GCD tests at 35 mA cm⁻² for continuous 5000 cycles.

**Figure 7.** Cycling performance of the C-Ni-4-Co-8 electrode at a discharge current density of 35 mA cm⁻².

As revealed in Fig. 7, a slightly increase of the capacitance is observed in the first 1000 cycles, which is most likely due to the electrolyte ions were immersed in the interior of the electrode

continuously and further activation of the electrochemical performance during the cycling process. Then, the capacitance of this electrode slowly reduced but still remains about 83% of its original capacitance after 5000 cycles, which demonstrated the excellent electrochemical stability of the C-Ni-4-Co-8 electrode.

4. CONCLUSIONS

In summary, a cost-effective hydrothermal synthesis method was used for fabricating the nickel-cobalt double hydroxides on carbonized cotton cloth, and it was directly used as binder-free electrodes. The controllable morphologies of NC-DH and three dimensional frameworks of carbon cloth provided numerous electroactive sites and accessible channels for electron transport, which contributed to provide short diffusion distance for electrolyte ions and fast redox reaction. The binder-free electrodes could ensure good electrical contact between the active materials and the current collector and improve the electrochemical properties. The C-Ni-4-Co-8 electrode had an optimum capacitance property, and the specific capacitance reached 4.19 F cm^{-2} when the current density was 5 mA cm^{-2} , and it also displayed a good rate capability of 3.05 F cm^{-2} even at a high current density of 80 mA cm^{-2} . In addition, the capacitance retention of electrode was up to 83% after charge/discharge 5000 cycles at 35 mA cm^{-2} . Such electrode exhibited remarkable electrochemical performance, particularly at a high current density, which meant its prospect application as the electrode materials for supercapacitors.

ACKNOWLEDGEMENTS

This research was supported by the Science & Technology Development Fund of Tianjin Education Commission for Higher Education (2018KJ202).

References

1. Z. Niu, W. Zhou, X. Chen, J. Chen and S. Xie, *Adv. Mater.*, 27(2015)6002.
2. Y. Wang, Y. Song and Y. Xia, *Chem. Soc. Rev.*, 45(2016)5925.
3. X. Peng, L. Peng, C. Wu and Y. Xie, *Chem. Soc. Rev.*, 43(2014)3303.
4. L. Dong, C. Xu, Y. Li, Z.H. Huang, F. Kang, Q.H. Yang and X. Zhao, *J. Mater. Chem. A*, 4(2016)4659.
5. M. Yousaf, H.T.H. Shi, Y. Wang, Y. Chen, Z. Ma, A. Cao, H.E. Naguib and R.P.S Han, *Adv. Energy Mater.*, 6(2016)1600490.
6. M. Sevilla and R Mokaya, *Energy Environ. Sci.*, 7(2014)1250.
7. L. Liu, Z. Niu and J. Chen, *Chem. Soc. Rev.*, 45(2016)4340.
8. Z. Zhang, Y. Zhang, X. Mu, J. Du, H. Wang, B. Huang, J. Zhou, X. Pan and E. Xie, *Electrochim. Acta*, 242(2017)100.
9. B. Mendoza-Sanchez and Y. Gogotsi, *Adv. Mater.*, 28(2016)6104.
10. Z. Huang, Z. Zhang, X. Qi, X. Ren, G. Xu, P. Wan, X. Sun and H. Zhang, *Nanoscale*, 8(2016)13273.
11. X. Shao, X. Zheng, W. Zou, Y. Luo, Q. Cen, Q. Ye, X. Xu and F. Wang, *Electrochim. Acta*,

- 248(2017)322.
12. C. Duan, J. Zhao, L. Qin, L. Yang and Y. Zhou, *Mater. Lett.*, 208(2017)65.
 13. G. Wang, H. Jia, L. Zhu, M. Li, Y. Ren and Y. Wang, *Int. J. Electrochem. Sci.*, 12(2017)3589.
 14. M. Jana, S. Saha, P. Samanta, N.C. Murmu, N.H. Kim, T. Kuila and J.H. Lee, *J. Mater. Chem. A*, 4(2016)2188.
 15. X. Sun, G. Wang, H. Sun, F. Lu, M. Yu and J. Lian, *J. Power Sources*, 238(2013)150.
 16. Y. Tang, Y. Liu, W. Guo, S. Yu and F. Gao, *Ionics*, 21(2015)1655.
 17. Z. Hu, Y. Xie, Y. Wang, H. Wu, Y. Yang and Z. Zhang, *Electrochim. Acta*, 54(2009)2737.
 18. H. Chen, F. Cai, Y. Kang, S. Zeng, M. Chen and Q. Li, *ACS Appl. Mater. Interfaces*, 6(2014)19630.
 19. X. Bai, Q. Liu, H. Zhang, J. Liu, Z. Li, X. Jing, Y. Yuan, L. Liu and J. Wang, *Electrochim. Acta*, 215(2016)492.
 20. G. Wang, H. Wang, X. Lu, Y. Ling, M. Yu, T. Zhai, Y. Tong and Y. Li, *Adv. Mater.*, 26(2014)2676.
 21. P.A. Shinde, V.C. Lokhande, T. Ji and C.D. Lokhande, *J. Colloid Interface Sci.*, 498(2017)202.
 22. L. Shi, P. Sun, L. Du, R. Xu, H. He, S. Tan, C. Zhao, L. Huang and W. Mai, *Mater. Lett.*, 175(2016),275.
 23. H. Chi, S. Tian, X. Hu, H. Qin and J. Xi, *J. Alloy Compd.*, 587(2014)354.
 24. S. Li, C. Yu, J. Yang, C. Zhao, M. Zhang, H. Huang, Z. Liu, W. Guo and J. Qiu, *Energy Environ. Sci.*, 10(2017)1958.
 25. U.M. Patil, J.S. Sohn, S.B. Kulkarni, S.C. Lee, H.G. Park, K.V. Gurav, J.H. Kim and S.C. Jun, *ACS Appl. Mater. Interfaces*, 6(2014)2450.
 26. H. Chen, L. Hu, M. Chen, Y. Yan and L. Wu, *Adv. Funct. Mater.*, 24(2014)934.
 27. T. Li, W. Zhang, L. Zhi, H. Yu, L. Dang, F. Shi, H. Xu, F. Hu, Z. Liu, Z. Lei and J. Qiu, *Nano Energy*, 30(2016)9.
 28. Z. Lv, Q. Zhong and Y. Bu, *Electrochim. Acta*, 215(2016)500.
 29. M.F. Warsi, I. Shakir, M. Shahid, M. Sarfraz, M. Nadeem and Z.A. Gilani, *Electrochim. Acta*, 135(2014)513.
 30. S.G. Kandalkar, H.M. Lee, S.H. Seo, K. Lee and C.K. Kim, *J. Mater. Sci.*, 46(2011)2977.
 31. W. Wei, W. Chen, L. Ding, S. Cui and L. Mi, *Nano Res.*, 10(2017)3726.
 32. D. Guo, X. Yu, W. Shi, Y. Luo, Q. Li and T. Wang, *J. Mater. Chem. A*, 2(2014)8833.
 33. Q. Zhang, N. Wang, P. Zhao, M. Yao and W. Hu, *J. Mater. Sci.*, 53(2018)14573.
 34. Q. Chen, H. Li, C. Cai, S. Yang, K. Huang, X. Wei, and J. Zhong, *RSC Adv.*, 3(2013)22922.
 35. J. Xiao, L. Wan, S. Yang, F. Xiao and S. Wang, *Nano Lett.*, 14(2014)831.
 36. P. Xu, W. Zeng, S. Luo, C. Ling, J. Xiao, A. Zhou, Y. Sun and K. Liao, *Electrochim. Acta*, 241(2017)41.